Research Article

Comparative analysis of fouling resistance prediction in shell and tube heat exchangers using advanced machine learning techniques

Kouidri Ikram[*1,a], Kaidameur Djilali[1,b], Dahmani Abdennasser[1, 2,c], Raheem Al-Sabur[3,d], Benyekhlef Ahmed[2,e], Abdel-Nasser Sharkawy[4, 5,f]

[1]*Dept. of Mechanical Eng., GIDD Industrial Engineering and Sustainable Development Laboratory, Faculty of Science and Technology, University of Relizane, Algeria*
[2]*Laboratory of Biomaterials and Transport Phenomena (LBMPT), University of Medea, Algeria*
[3] *Dept. of Mechanical Eng., College of Engineering, University of Basrah, Basrah 61001, Iraq*
[4] *Dept. of Mechanical Eng., Faculty of Engineering, South Valley University, Qena 83523, Egypt*
[5] *Dept. of Mechanical Eng., College of Engineering, Fahad Bin Sultan University, Tabuk 47721, Saudi Arabia*

Article Info	Abstract
	Heat exchangers are utilized in a vast region of the process industry for heating and cooling. Long-term operation of heat exchangers results in decreased efficiency due to many problems, such as fouling. Therefore, the object of this research paper is to use three artificial intelligence techniques (feedforward neural networks-multilayer perceptron (FNN-MLP), nonlinear autoregressive networks with exogenous inputs (NARX), and support vector machines (SVM-RBF)) for predicting the fouling resistance in the tube and the shell heat exchanger in the preheating circuit of atmospheric distillation. The results summarize the high training as well as the predictive capacity of the "FFNN-MLP" model for predicting the fouling resistance in the heat exchanger with the highest coefficient of correlation (R = 0.99961) and the lowest root-mean-squared error (nRMSE = 1.0031%) for the testing phase, where the FNN-MLP network is superior to that provided using the SVM model (R = 0.9955 and nRMSE = 3.8652%). All the models of artificial networks and machine learning techniques used in the current work can be used to predict the fouling resistance in heat exchanger data with high accuracy. Despite this, the FNN-MLP model is the preferred model compared with the other proposed models, followed by the NARX model.

1. Introduction

The heat exchanger (HE) is an essential equipment widely used in considerable industrial applications such as power production, heating and refrigeration, petroleum and chemical industry, food processing, and waste heat recovery [1], [2]. Usually, around 90% of the thermal industrial operations pass in a heat exchanger at least once [3]. It ensures heat transfer occurs between two fluids at different temperatures. Also, it can transmit energy in the form of latent heat, such as in condensers and boilers, or sensible heat, such as in coolers and heaters [4]. Heat exchangers are categorized based on the principal using criteria such as transfer processes, quantity of fluids, surface compactness, construction characteristics, heat transfer methods, and flow arrangements [5]. Among various classifications of HE, shell and tube heat types are the most often utilized in industrial applications. In this exchanger, the tubes are arranged according to different motifs [6].

[*]Corresponding author: kouidri.ikram@univ-relizane.dz
[a]orcid.org/0009-0008-7989-7610, [b]orcid.org/0000-0003-3294-9395, [c]orcid.org/0000-0002-8473-7127, [d] orcid.org/0000-0003-1012-7681, [e] orcid.org/0000-0002-0881-9358, [f] orcid.org/0000-0001-9733-221X

In contrast, several baffles are usually added at a uniform spacing inside the shell to increase turbulence and improve heat transfer. The flow can be parallel, counter, or sometimes crossed [7]. Despite their advantages, heat exchangers' performance declines dramatically with age of exchangers, and many problems arise, especially vibration and fouling. The poor quality of the media used, especially on the tube side, can lead to increased fouling problems and decrease the exchanger's performance, even in short periods. A fouling phenomenon occurs when unwanted deposits accumulate on the heat transfer surfaces in heat exchanges over time. This phenomenon leads to operational inefficiencies and increases energy consumption. So, accurate prediction of fouling resistance is a crucial goal for many industries.

Sediments, crystals, and biological residues are familiar forms of fouling and can be extended to the products of a chemical reaction or even the combination of several of these elements. This deposit, developed on one side or both sides of the heat exchange surface, has poorer thermal conductivity than the metal comprising the exchange surface, resulting in a high increase in total resistance [8]. The fouling results are the main reason for the decrease in heat transfer coefficients, as are changes in the surface's topography and the flow's geometry. Furthermore, significant pressure reductions occur due to the constriction of flow and increased friction caused by scale development that can render a heat exchanger unusable even before the lowered thermal efficiency [9], [10]. Many aspects influence the development of fouling, including fluid composition, operating conditions, heat exchanger type and features, and fouling site [11]. As a result, considering all these variables makes it impossible to build a semi-empirical or empirical connection to predict the fouling factor precisely [12]. Accurately predicting fouling resistance is essential for optimizing heat exchanger performance, reducing downtime, and minimizing maintenance costs.

Fouling prediction is a primary goal for many researchers, and the methods that can be used for this purpose have varied. It is worth noting that experiments, computational fluid dynamics (CFD) simulations, and other traditional methods failed due to many considerations, including time, resources, and accuracy in predicting the effects of fouling. Accordingly, research institutions have turned to more appropriate patterns, such as machine learning algorithms, to predict the fouling resistance.

Rached Ben-Mansour et al. [13] explored and discussed the fouling analysis in several previous studies on various types of heat exchangers, especially those considering thermal desalination systems. Xiao Zheng et al. [14] used regression neural network (GRNN) as well as random forests (RF) algorithms to predict the coefficient of heat transfer in channels of heat exchange with the effect of bulges in many locations on HTC as input data and 143 set data. They concluded that the GRNN model is better than the RF algorithm in the heat transfer channels' prediction accuracy and generalization ability. Jyoti Prakash Panda et al. [15] modeled the heat transfer correlations for the twisted tape heat exchangers. Artificial neural network (ANN), random forest (RF), and polynomial regression are employed for surrogate modeling. The input data are the Reynolds numbers, the twist ratio, the perforation percentage, and the different numbers of the twisted tapes. This study concluded that the potential ANN is suitable for future data-driven modeling. Anurag Kumra et al. [16] used the SVM and ANN models for predicting the heat transfer rate in wire-on-tube type heat exchangers, they used the flow direction, heat transfer surfaces area, diameter, volumetric flow rate, mass flow rate, and temperature as input values. The results showed that the SVM modeling approach provides better performance and more precise results. Wen et al. [17] indicated that the vector regression machine (SVR) approach outperformed the partial least squares (PLS) algorithm for predicting the fouling in the plate heat exchanger. They used the input data of pH, dissolved oxygen, chloride ion, iron ion, conductivity, dissolved, hardness, turbidity, alkalinity, and the total bacterial

count. In the same direction, Wen Xiaoqiang et al.[18] the multi-resolution wavelet neural network (MRWNN) exceeds other neural networks according to its significance in nonlinear function approximations. Aminian and Shahhosseini [19] tried to avoid the operating conditions that accelerate fouling in pre-heat exchangers by using ANN to develop the mathematical formulation sets. Seyit Ahmet Kuzucanlı et al. [20] examined several multi-classification algorithms and compared them to predict the fouling resistance and the overall heat transfer coefficient in plate heat exchangers. They found that the Naïve Bayes algorithm was better than the decision tree algorithm and k-nearest neighbors (kNN). Sreenath Sundar et al. [21] found that using a robust algorithmic framework for deep learning non-linear functional relationships is suitable for predicting the fouling of the waste heat recovery crossflow heat exchanger. Also, they found that multiple ANNs attain more reasonable accuracy and robustness to noise. Sun Lingfang et al. [22]used the SVM and the wavelet relevance vector machine [23] to predict the fouling resistance in heat exchangers based on the statistical learning theory. They found that the SVM model indicates high prediction accuracy.

More specifically, some studies have been concerned with predicting fouling resistance in shell and tube heat types. Emad M.S. El-Said et al. [24] utilized social media optimization (SMO), k-nearest neighbors' algorithm (KNN), SVM, random vector functional link (RVFL) algorithms to predict the outlet temperature and pressure drop values, and they found that the RVFL outperformed other algorithms. Cao Shengxian et al. [25] indicated that the least squares-support vector machine (LS-SVM) and the BP neural network algorithms have better accuracies than traditional methods for predicting cooling water biofouling resistance. They considered pH, conductivity, total number of bacteria, dissolved oxygen, TN, and NH3-N as input parameters. R. Harche et al. [26] employed long-short-term memory (LSTM) and random forest (RF) to predict fouling status according to historical data in crude distillation unit preheat trains in petroleum refineries. Al-Naser et al. [27] also used LSTM and the ANN in two stages to calculate the fouling factor of the shell and tube heat exchangers using commercial software, and they found the prediction accuracy to be very high. Later, Al-Naser et al. [28] expanded their study from fouling prediction to estimating the local fouling factor using an artificial model of different fouling tactics simulations.

Providing accurate and robust results to predict fouling resistance in heat exchangers is one of the limitations in recent years when using traditional methods, where the results are far from practical reality. Therefore, researchers' growing consensus emerged regarding the need for advanced artificial intelligence (AI) models because they possess excellent capabilities, such as dealing with complex and non-linear patterns. These techniques have become the most promising comprehensive comparative analysis method. This study highlights the importance of advanced artificial intelligence models in predicting fouling resistance in shell-and-tube heat exchangers.

In the realm of heat exchanger research, there exists a notable research gap regarding the comprehensive exploration of three distinct artificial intelligence techniques, namely feedforward neural networks-multilayer perceptron (FNN-MLP), a nonlinear autoregressive model with exogenous inputs (NARX), and the support vector machine (SVM), in predicting fouling resistance. Their application to shell and tube heat exchangers has remained largely uncharted territory. This study endeavours to bridge this research gap by offering a comprehensive investigation into the prediction of fouling resistance through an extensive comparison of FNN-MLP, NARX, and SVM-RBF methods. Furthermore, we aim to present the outcomes of our research in a manner that facilitates their practical implementation in the real world, drawing upon experimental data from a refinery in Algeria. By addressing this research gap, our work seeks to contribute

significantly to resolving a longstanding industrial challenge in heat exchangers, particularly within the shell and tube configurations domain.

2. Materials and Methods

2.1. Data Acquisition and Preprocessing for Experimental Analysis

Atmospheric distillation (U100) is the basic unit of an ALGIERS refinery. It aims to split crude oil into various finished products (kerosene, diesel, fuel oil, LPG, and light and heavy solvents), which can be used for one or more treatments. For our study, we are interested in the preheating circuit of this unit when the crude oil leaves the storage bins at room temperature; it is discharged by one of three pumps of type centrifugal, P101, to the atmospheric distillation unit, then passes through two circuits of E101 battery (FED and CBA). Crude oil passes through the battery on the tube side, where it is heated with head reflux (RT), the light product mixture from the top of the C101 distillation column at tray 46. The oil then passes through electrostatic desalination by treating the water with caustic soda. This treated water is injected at the E101 heat exchanger inlet and at the desalted entrance to wash the crude oil and drive the salts present (Fig.1).
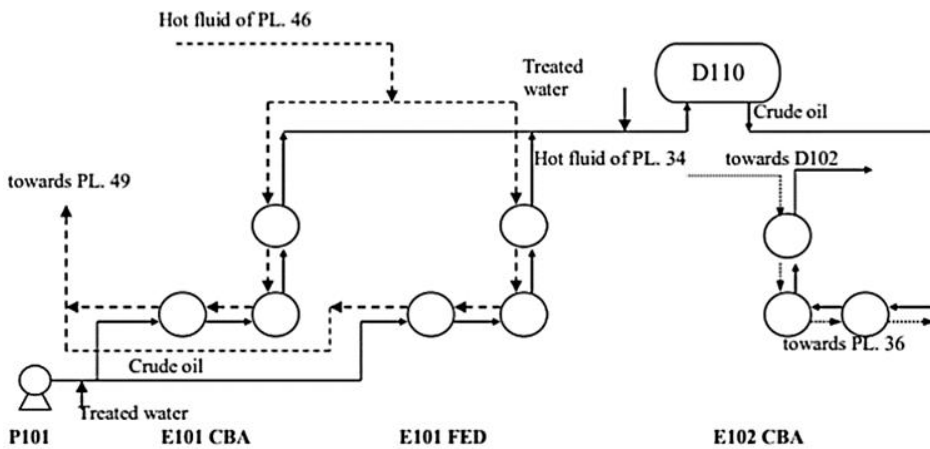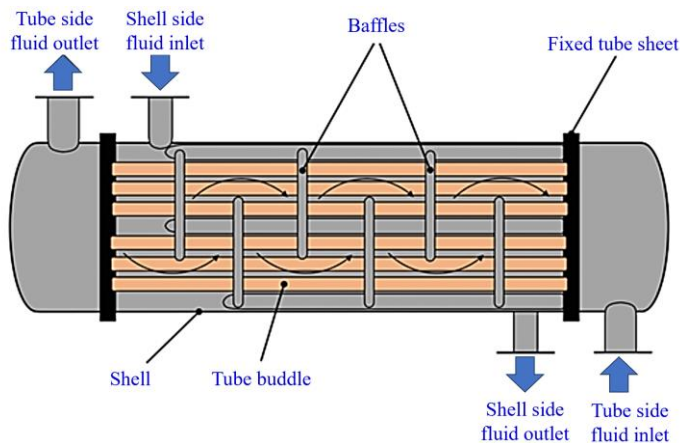

Fig. 1 Atmospheric distillation scheme (unit 100) [26]

Fig. 2 Shell and tube heat exchanger

4

This work primarily aims to verify the performance measure of the E101 CBA heat exchanger by predicting the fouling resistance. E101CBA is a shell and tube exchanger with one pass on the shell and two on the tube sides. Fig. 2 illustrates the main parts of the shell and tube heat exchanger. Crude oil passes through the tubes while head reflux (RT) flows in the shell side. Several sensors are placed to measure flow rates and temperatures. Table 1. presents the measured variables of the E101CBA heat exchanger. Standard deviations (SD) were added to explore the process variables' variation.

Table 1. Statistical analysis for shell and tube process parameters

Side	Parameters	Unit	Min	Mean	Max	SD
Tube	Inlet Temperature (t_i)	°C	17	24	31	4.169
	Outlet Temperature (t_o)	°C	101	92	110	2.367
	Mass flux ($\dot{m}_t$)	Kg/s	23.50	34.80	46.10	6.009
Shell	Inlet Temperature (T_i)	°C	111	120.5	130	3.253
	Outlet Temperature (T_o)	°C	44	54	64	4.528
	Mass flux ($\dot{m}_s$)	Kg/s	38.98	59.54	80.104	6.560
	Fouling resistance (R_f)	m²°C/W	0.00017	0.0093	0.0017	0.003

2.2. Feed-forward Multi-layer Perceptron

The most often utilized architecture now is the multilayer-feedforward neural network, referred to as the multi-layer perceptron (MLP) network [29]. This structure comprises the hidden layer or layers, the output layer, and the input layer. A nonlinear input-output model structure can be considered this kind of network. This network passes signals from one node to each subsequent layer's nodes [30]. The multi-layer feed-forward neural network's topology is shown in Fig. 3. This picture shows how the input layer receives all the input signals and transfers them to additional neurons in the hidden layer, where the processing task is carried out. The output layer then receives the data. Synaptic weights and biases are the parameters of such a network.
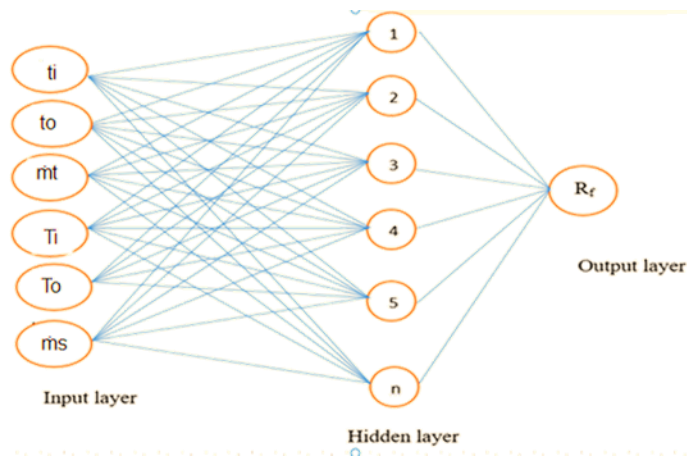

Fig. 3 Multilayer feedforward neural network's topology

The outputs of the FNN are the outcomes of the neuromorphic model. The output of the proposed MLP neural network can be given as follows [31]:

$$y_i = Qi(\sum_{j-1}^{n^i} W_j^i Z_j^i + b^i)$$

(1)

The activation function Qi regulates the i-th node's output within a specific range, which depends on the total incoming connections n^i, bias bi, weight Wi, and input Zi.

2.3. Nonlinear Autoregressive Models with Exogenous Inputs (NARX)

The NARX network [32], [33] is the recurrent ANN with feedback connections enclosing many network layers. This model has the well-known ARX model nonlinear generalization. In addition, it predicts the time series in a very efficient way [34], [35]. This model is used widely with nonlinear systems [36], [37]. The NARXNN model consists of three layers, as indicated in Fig. 4. The input layer consists of six parameters (mentioned before), a nonlinear hidden layer that contains the hidden neurons and its activation function of type hyperbolic tangent, tanh. In contrast, the third layer represents the nonlinear output which estimates the fouling resistance. The activation function in the output layer is the hyperbolic tangent, tanh. The vector of the input delay is [0 1], whereas the vector of the output delay is [1 2].
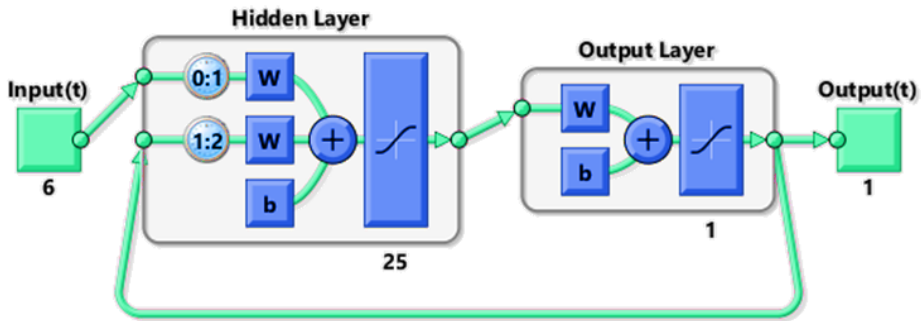

Fig. 4 The designed and proposed NARX network architecture

2.4. Support Vector Machine

The SVM technique is a collection of supervised learning strategies designed to address discrimination and regression issues [38]. Due to its capacity to handle vast amounts of data, SVM gained popularity quickly [39]. The SVM implements nonlinear class borders using some input vectors of nonlinear mapping into the high-dimensional feature space and then uses a linear model to generate a hyperplane. The Radial basis function kernel (RBF kernel) is a well-liked kernel function in support vector machine classification [40].

The output of an SVM model can be determined by solving a specific equation (2):

$$f(x_i) = \omega^T \emptyset(x_i) + b, i = 1,2, \dots, n$$

(2)

Where $f(x_i)$ refers to the predicted data, $\varphi(x_i)$ is the implicitly constructed nonlinear function, ω is the SVM model's weight vector, and b is the SVM model's bias. The dataset has the D-dimensional input vector $x_i \in R^D$ and the scalar output $y_i \in R$.

2.5. Assessment Performance Evaluation

Several error measures were employed to control the prediction models' precision level. These error measures include the Coefficient of Correlation (R), Mean Absolute Error

(nMAE), Root mean squared error (nRMSE), and standard prediction error (SEP). Equations that specify these errors mathematically represent the equations (3–7) [41], [42]. These error measurements make it possible to evaluate the performance of the prediction models in detail and get a good grasp of their advantages and disadvantages.

y and y' are the measured and calculated values of the fouling resistance in the tube and the shell heat exchanger; their mean values are:

$$\bar{y} = \sum_{i=1}^{N} y_i/N \quad \text{and} \quad \bar{y}' = \sum_{i=1}^{N} y_i'/N \quad \text{where N is the data number}$$

$$R = \frac{\sum_{i=1}^{n} \left(Y_{i,exp} - \overline{Y_{i,exp}}\right)\left(Y_{i,cal} - \overline{Y_{i,cal}}\right)}{\sqrt{\sum_{i=1}^{n} \left(Y_{i,exp} - \overline{Y_{i,exp}}\right)^2 \sum_{i=1}^{n} \left(Y_{i,cal} - \overline{Y_{i,cal}}\right)^2}} \qquad (3)$$

The mean absolute error, MAE, as well as its normalized value, nMAE:

$$MAE = \frac{1}{n}\sum_{i=1}^{n} \left|Y_{i,cal} - Y_{i,exp}\right| \quad ; \quad nMAE = MAE/\bar{y} \qquad (4)$$

The root-mean-square error, RMSE, as well as its normalized value, nRMSE:

$$RMSE = \sqrt{\frac{\sum_{i=1}^{n} (Y_{i,cal} - Y_{i,exp})^2}{n}} \qquad ; \quad nRMSE = RMSE/\bar{y} \qquad (5)$$

$$SEP(\%) = \frac{RMSE}{Y_e} \times 100 \qquad (6)$$

Concerning a dataset comprising n data points, where $Y_{i,exp}$, and $Y_{i,cal}$ correspond for the experimental and calculated fouling resistance values, and $\overline{Y}_{i,exp}$ represents the mean of experimental data.

3. Results and Discussion

3.1. The Database's Division's Impact

The entire database was divided into three sections to assess the performance of the three models: FFNN-MLP, SVM-RBF, and NARX. Section 1 had 174 training points (60%) and 116 for testing (40%); Section 2 had 203 points for training (70%); and Section 3 had 232 points for training (80%) and 58 for testing (20%). Table 2 presents the correlation coefficient (R) and the normalized root-mean-squared error (nRMSE) for predicting fouling resistance considering the database impact's division. The results show that the third section is the best division, giving better results than the other divisions for the test and training phases. The three models (SVM-RBF, FFNN-MLP, and NARX model) were used for predicting fouling resistance and compared with each other.

In this study, the BFGS quasi-Newton [trainbfg] was used as the training algorithm for FNN-MLP, and Levenberg-Marquardt (LM) for NARX, while the Radial basis function (RBF) was used for the radial basis function (RBF).

Table 2. Impact of the database's partition for FNN-MLP

| Partitions	Database	%	nRMSE	R
1	Training: 174 points	60%	1.5970	0.99872
	Testing: 116 points	40%	1.3991	0.99904
2	Training: 203 points	70%	1.3884	0.99901
	Testing: 87 points	30%	1.3630	0.99916
3	Training: 232 points	80%	0.9694	0.99951
	Testing: 58 points	20%	1.0031	0.99961

3.2. FNN-MLP Model

The NN architecture for predicting fouling resistance was optimized using STATISTICA software, and this study uses the BFGS quasi-Newton, trainbfg, training algorithm. The optimal structure of the (FNN-MLP) model used to predict fouling resistance is the more detailed architecture presented in Table 3.

Table 3. The main structure of the developed FNN-MLP network

Training Technique	Input layer	Hidden layer		Output layer	
BFGS quasi-Newton (trainbfg)	Neurons	Neurons	Activation function	Neurons	Activation function
	06	20	Exponential	1	Sine

The agreement between experimental and calculated fouling resistance in heat exchangers obtained by the FNN-MLP model optimal is excellent, with agreed vectors about the ideal [a (the slope), (y-intercept), (correlation coefficient)] = [0.9985, 1.50750, 0.99951] in the training phase and [a, b, R] = [1.0012, -1.52666, 0.99961] in the test phase (Fig. 5).

(a)   (b)
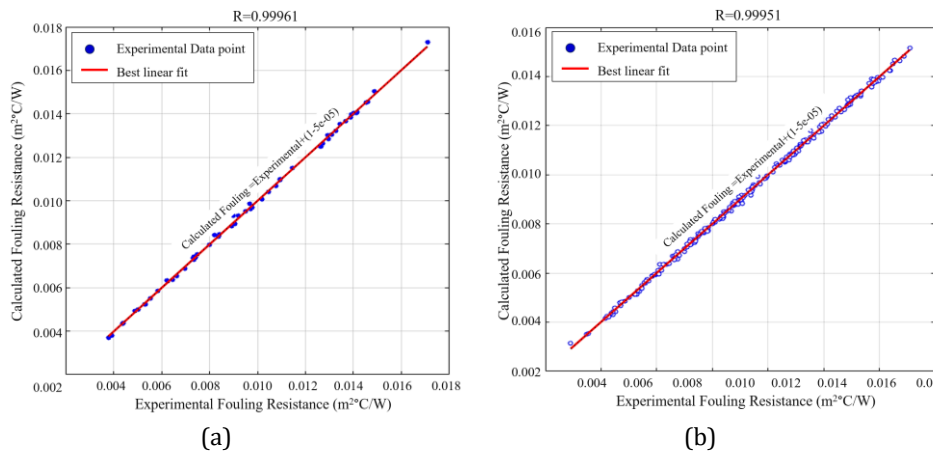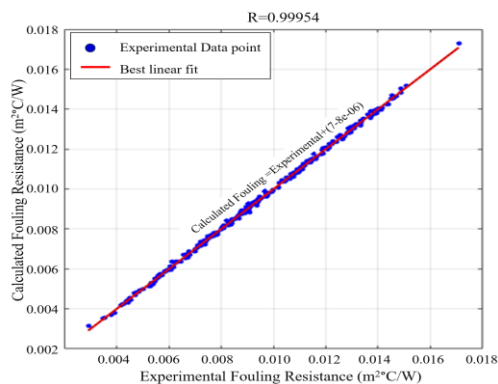
(c)

Fig. 5 FNN-MLP Model Experimental vs. calculated fouling resistance: (a) train dataset, (b) test dataset, (c) total dataset

3.3. NARX Model

The NARX neural network architecture for predicting fouling resistance was optimized using MATLAB software; this study uses the Levenberg-Marquardt (LM) training algorithm. Intel(R) Core (TM) i5-8250U CPU @ 1.60GHz processor is used for this network. The optimal structure of the NARX model used to predict fouling resistance is the more detailed structure presented in Table 4.

Table 4. Structure of the developed NARX model

Training Technique	Input layer	Hidden layer		Output layer	
the Levenberg-Marquardt (LM)	Neurons	Neurons	Activation function	Neurons	Activation function
	06	25	Hyperbolic Tangent (Tanh)	1	Hyperbolic Tangent (Tanh)

The number of layers was similar for input, hidden, and output, where it was one layer. The number of neurons in the input and hidden layers was 6 and 25, respectively, while it was 1 for the output layer.

The choice of hyperbolic tangent activation function allows the neural network models to capture complex, nonlinear relationships within the fouling resistance prediction problem. By utilizing the hyperbolic tangent activation function, the selected models can effectively comprehend and represent intricate patterns in the data, enhancing their predictive abilities.

The agreement between experimental and calculated fouling resistance in heat exchangers obtained by the optimal NARX model is excellent. The obtained regression and mean squared error (MSE) in the training and testing cases are presented in Fig. 6 and 7. The best-obtained value is 1.9318e-08 at epoch 26, a minimal value and about zero.
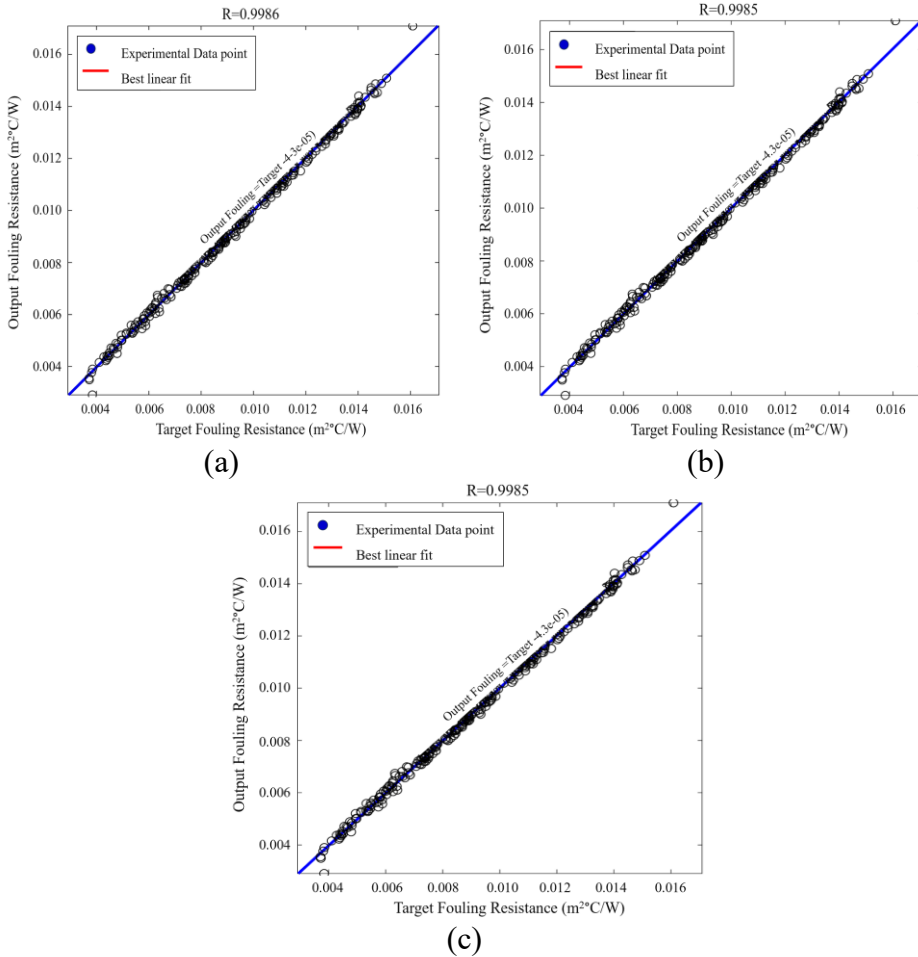
Fig. 6 NARX model Experimental vs. calculated fouling resistance: (a) train dataset, (b) test dataset, (c) total dataset
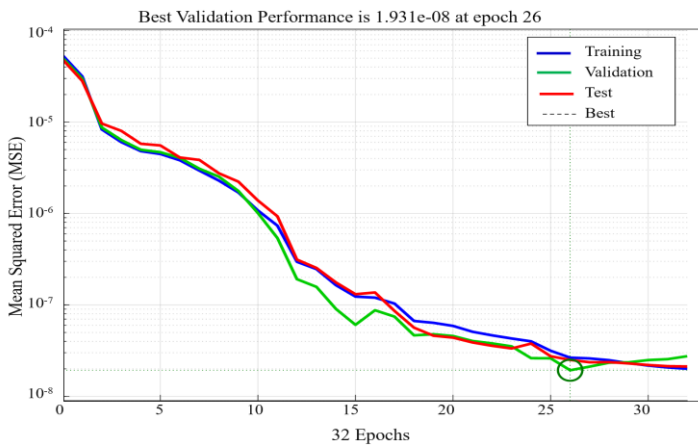

Fig. 7 MSE for the training, testing, and validation of the NARX model

The experimental fouling resistance from these Figures coincides and converges with the estimated one by the NARX neural network, where the obtained MSE is minimal and close to zero. In other words, the NARX model is an effective and perfect training method. Moreover, the experimental and the calculated fouling resistance were compared, as shown in Fig. 8. The results refer to perfect convergence and coinciding, which supports the fact that the NARX model works excellently.
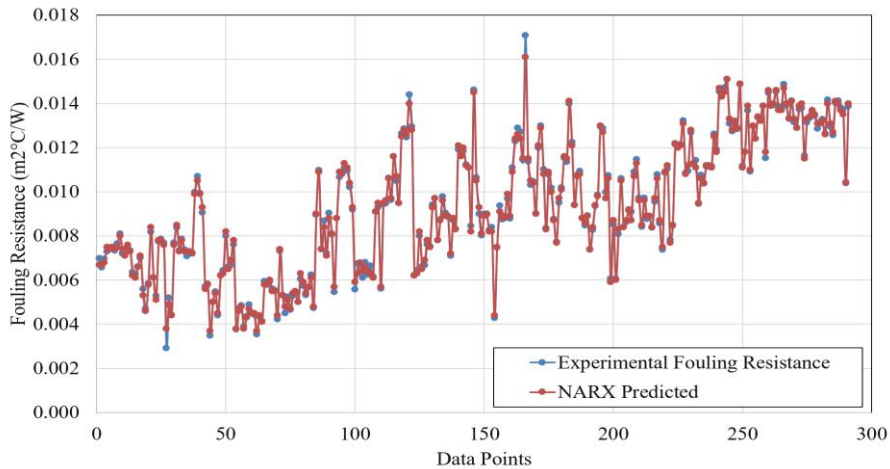

Fig. 8 Experimental fouling resistance and NARX model predicted comparison using all data

3.4. SVM-RBF Model

The SVM-RBF network gives a relationship of type nonlinear between the inputs (ti, to, ṁt, Ti, To, ṁs) and the output (fouling resistance). For the prediction of the fouling resistance in the E101CBA heat exchanger using the SVM-RBF model, the same database used in the FNN-MLP model was selected. Table 5 shows the evaluation of the SVM-RBF model in terms of the number of support vector machines (N° SV), nRMSE, and R. The nRMSE of the SVM-RBF is 3.2591 %, 3.8652 %, and 3.3871 % for training, tasting, and overall phases, respectively. The SVM-RBF model's correlation coefficients for training, testing, and overall phases are 0.99555, 0.99551, and 0.99549, respectively. These correlation indices are getting near the ideal (R = 1). In addition, the RBF-kernel function is a better choice for describing the prediction of fouling resistance.

Table 5. Evaluation of SVM-RBF model

(SVM-RBF) model	N° SV	Phase	nRMSE	R
C (10.00)	120	Training	3.2591	0.99555
nu (0.500)		Testing	3.8652	0.99551
Gamma (0.150)		Overall	3.3871	0.99549

Fig. 9 indicates a high convergence of the predicted fouling resistance to experimental sets where it is near ideal behavior (slope = 1, intercept = 0, R = 1). The correlation coefficient R and nRMSE results showed that the SVM-RBF model operated somewhat during the training and testing phases. Also, the overall phase shows the SVM-RBF model's predictive power, closely following the trend of the experimental data on fouling resistance, except in

a few instances where the differences between experimental and predicted values are notable.
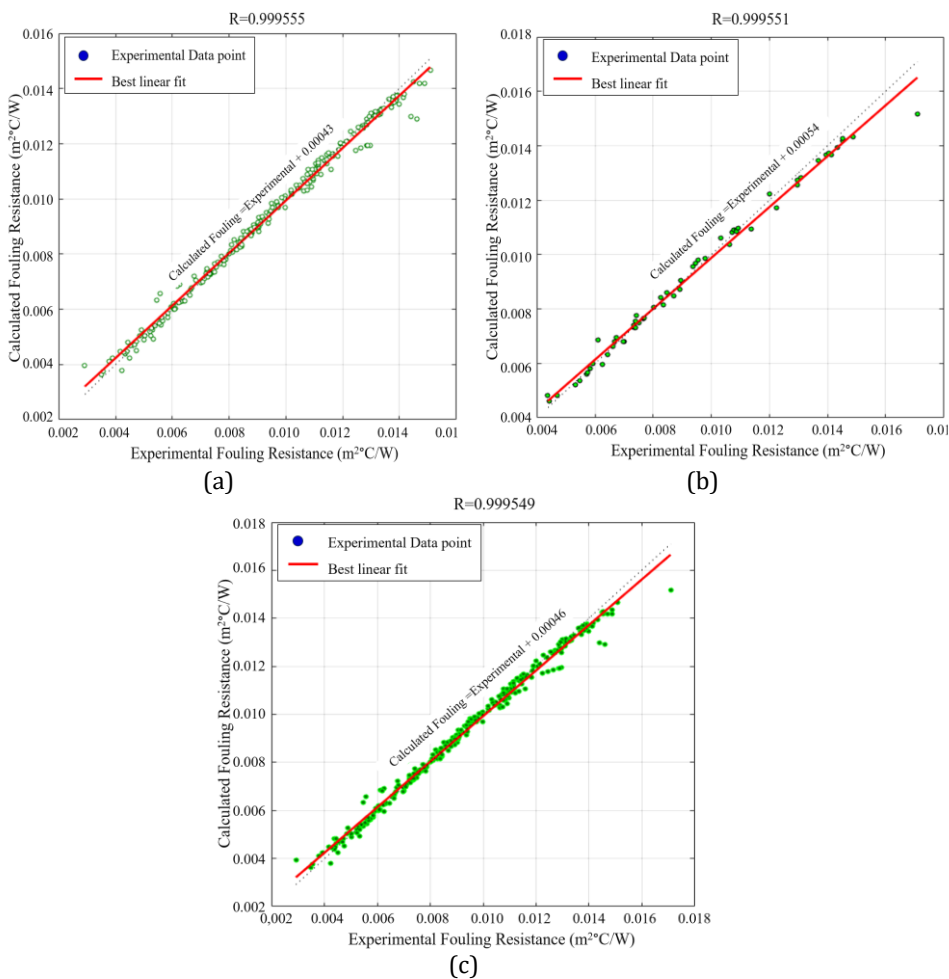

(a)

(b)

(c)

Fig. 9 SVM-RBF model Experimental vs. calculated fouling resistance: (a) train dataset, (b) test dataset, (c) total dataset

The results show that the FNN-MLP and the NARX models acquired the lowest nMAE, nRMSE, and SEP errors in the testing phase (0.7939, 1.0031, and 1.0027, respectively). It can be observed clearly in Table 6 that the FNN-MLP and the NARX-based models surpassed the SVM-RBF and RF models for predicting resistance to fouling.

Table 6. The statistical evaluation of the model's performance

Errors	FNN-MLP		NARX		SVM-RBF	
	Training	Testing	Training	Testing	Training	Testing
R	0.99951	0.99961	0.9986	0.9985	0.9956	0.9955
nMAE (%)	0.7706	0.7939	1.2589	1.2723	2.0541	2.4982
nRMSE (%)	0.9694	1.0031	1.3611	1.4231	3.2591	3.8652
SEP (%)	0.9696	1.0027	1.3508	1.4101	3.2497	3.8340

3.5. Sensitivity Analysis

A sensitivity analysis employing the "Weight" approach was used to examine the impact of the input variables (Inlet Temperature, Outlet Temperature, Mass Flow in the Tube Side and Shell Side) on the output (fouling resistance).

The "weight approach" in the sensitivity analysis was first used in the early 1990s by Garson [43] and then developed by Goh [44] to be widely used. It is usually used in experiments to give the relative significance (RI) of the input to the output of a neural network. It depends on dividing the connection's weights into the input-hidden connection's weights and the hidden-output connection's weights. Fig. 10 displays the contribution results. The most crucial variables that may affect the prediction of resistance fouling are the crude oil outlet temperature of 26.56% and the head reflux outlet temperature of 15.46%. The contributions of head reflux inlet temperature, crude oil inlet temperature, and head reflux Mass flux are not significantly different (almost the same contribution with RI = 15%), and crude oil mass flux has less effect with RI = 13%. Results of the sensitivity analysis show that all input parameters have a relative importance higher than > 12%, which explains the effect of the selected parameters on the output.
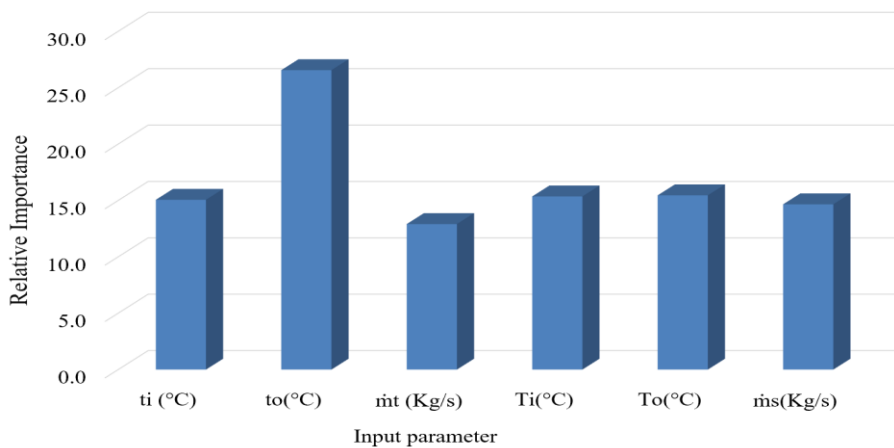

Fig. 10 Relative importance (%) of input variables on fouling resistance

3.6. Comparison with Other Models

Comparisons with similar studies are crucial to the value of scientific research and give it the value of originality. Table 7 compares a specific category of previous studies that are similar or close in their input parameters to the current study—all selected studies aimed at predicting heat exchanger fouling. The comparative study indicates that FFNN-MLP and NARX represent the most accurate and reliable models in terms of predictive values.

This superiority of the FFNN-MLP and NARX models in predicting the fouling resistance of heat exchangers can be attributed to the theoretical foundations of these two methods. Both models are mainly designed to deal with complex nonlinear relationships, especially those in which time has a significant influence. Heat exchangers depend on a complex mixture of inputs that interfere with each other, especially after a period of use. Fouling in the heat exchanger accumulate with prolonged use, especially with poor maintenance, and meads, especially on the side of the tube. Therefore, FFNN-MLP and NARX can give better results with all these nonlinear parameters.

The results obtained gave a clearer view of the prediction of fouling resistance in the atmospheric distillation (U100), which is the basic unit of an ALGIERS refinery and helped workers obtain a better performance for treating water which is injected at the E101 heat exchanger inlet.

Table 7. Predicted fouling resistance comparison with previous studies

Ref	Input variables	Prediction Variable	Model Type	Errors "R, R^2, RMSE, MAE"
Present work	Inlet and outlet temperature of crude oil, mass flow of crude oil, inlet and outlet temperature of head reflux(RT) and mass flow of (RT)	Fouling resistance	FNN-MLP	R=0.99961 nRMSE=$1.0031*10^{-2}$ nMAE= $0.7939*10^{-2}$
			NARX	R=0.9985 nRMSE=$1.4231*10^{2}$ nMAE= $1.2723*10^{-2}$
			SVM-RBF	R=0.9955 nRMSE=$3.8652*10^{2}$ nMAE= $2.4982*10^{-2}$
[45]	Fluid temperature, surface temperature, operation time, fluid density, equivalent diameter, velocity, and oxygen content.	Fouling factor	GPR	R^2=0,98770 MSE=$8,53.10^{4}$ MAE=$5,35.10^{-3}$
			SVM	R^2=0,97702 MSE=$1,65.10^{-3}$ MAE=$1,5.10^{-2}$
			Decision trees	R^2=0,98664 MSE=$9,22.10^{-4}$ MAE=$8,84.10^{-3}$
			Bagged trees	R^2=0,98484 MSE=$1,15.10^{-3}$ MAE=$1,22.10^{-2}$
			Linear regression	R^2=0,57753 MSE=$4,98.10^{-2}$ MAE=$4,65.10^{-2}$
[46]	Feed water temperature and flow rate, flue gas inlet and outlet temperatures, blower A and B air supply rates, steam flow rate and oxygen amount	Ash fouling resistance	SVM	R=0,985 MSE=0.001126
[47]	Acid inlet and outlet temperature, acid volume flow and density, steam temperature and operation time.	Fouling resistance	ANN-MLP	R^2=0,995 MSE=$4.256×10^{-6}$
[12]	Fluid and surface temperatures, dissolved oxygen concentration, equivalent diameter, operation time, density, velocity.	Fouling resistance in heat exchanger	ANN-MLP	R^2=0,9778 MSE=0.0355
[48]	Coal ash composition and structure parameters	Fouling fact or index	ANN	R^2=0,9996 MSE=0,0073 MAE= $2.308.10^{-2}$

| [1] | Acid Inlet and outlet temperatures, density, flow rate, operation time, and steam temperature. | Fouling resistance | ANN | R^2=0,994 MSE=2.168 $\times$ 10^{-11} RMSE=4.656$\times$ 10^{-6} |
| [49] | Input temperature and flow rate of tube side, and input temperature of shell side. | Fouling resistance | ANN | MSE= 8, 06. 10^{-2} |

4. Conclusions

Heat exchanger modelling plays a very important role in the thermal analysis of heat exchangers. Artificial intelligence methods are powerful computer models that capture and represent complex input/output relationships.

The study focused on fouling resistance prediction using conventional machine learning models such as feedforward networks multi-layer perceptron, NARX model and support vector machine radial basis function kernel (FFNN-MLP, NARX, and SVM-RBF) with supervised learning. The results indicated the fouling resistance's high train and prediction capacity with a higher correlation coefficient (R = 0.99961) and a very low root mean squared error (nRMSE = 1.0031%) for the testing phase. The prediction by FFNN-MLP correspondingly demonstrates a sound correlation between the fouling resistance experimental and predicted values, indicating that the FFNN-MLP model has superior predictive power. The analysis of sensitivity was calculated and verified that fouling resistance in heat exchanger is handled by three interactions which were arranged in dropping order: Cold-Outlet Temperature (Relative Importance RI = 26.56%), Hot-Outlet Temperature (RI = 15.46%), Hot-Inlet Temperature (RI = 54.35%), Cold-Inlet Temperature (15.09), Hot-Mass flux and Cold-Mass flux (14.65% and 12.9%, respectively). Furthermore, the study suggests that the FFNN-MLP model can be applied to predict fouling resistance in EA 101CBA heat exchangers or similar character conditions.

In future work, other neural network approaches, such as Cascaded Forward NN, Radial basis function, and recurrent neural network, can be investigated. In addition, deep learning approaches will be investigated.

References

[1] Jradi R, Marvillet C, Jeday MR. Modeling and comparative study of heat exchangers fouling in phosphoric acid concentration plant using experimental data. Heat and Mass Transfer, 2020; 56:2653-2666. https://doi.org/10.1007/s00231-020-02888-9

[2] Faes W, Lecompte S, Ahmed ZY, Van Bael J, Salenbien R, Verbeken K, De Paepe M. Corrosion and corrosion prevention in heat exchangers. Corrosion reviews, 2019; 37(2): 131-155. https://doi.org/10.1515/corrrev-2018-0054

[3] Fguiri A, Jradi R, Marvillet C, Jeday MR. Heat exchangers fouling in phosphoric acid concentration. Heat and Mass Transfer, 2020; 56:2313-2324. https://doi.org/10.1007/s00231-020-02858-1

[4] Sulaiman MA, Kuye SI, Owolabi SA. Investigation of fouling effect on overall performance of shell and tube heat exchanger in a urea fertilizer production company in Nigeria. Nigerian Journal of Technology, 2016; 35(1): 129-136. https://doi.org/10.4314/njt.v35i1.20

[5] Abbas EF, Yagoob JA, Mardan MN. Effect of tube material on the fouling resistance in the heat exchanger. In 2nd International Conference for Engineering, Technology and Sciences of Al-Kitab University, Iraq ,43-48, December, 2018. https://doi.org/10.1109/ICETS.2018.8724619

[6] Musawel RK. (2002). Simulation and fouling study of propane heat exchangers, MSc Thesis, UNIVERSITY OF BASRAH, Iraq.

[7] Abd AA, Kareem MQ, Naji SZ. Performance analysis of shell and tube heat exchanger: Parametric study. Case Studies in Thermal Engineering, 2018; 12:563-568. https://doi.org/10.1016/j.csite.2018.07.009

[8] Fguiri A, Marvillet C, Jeday MR. Estimation of fouling resistance in a phosphoric acid/steam heat exchanger using inverse method. Applied Thermal Engineering, 2021; 192:116935. https://doi.org/10.1016/j.applthermaleng.2021.116935

[9] Emani S, Ramasamy M, Shaari KZBK. Effect of shear stress on crude oil fouling in a heat exchanger tube through CFD simulations. Procedia Engineering, 2016; 148:1058-1065. https://doi.org/10.1016/j.proeng.2016.06.592

[10] Berce J, Zupančič M, Može M, Golobič I. A review of crystallization fouling in heat exchangers. Processes, 2021; 9(8):1356. https://doi.org/10.3390/pr9081356

[11] Gudmundsson O, Palsson OP, Palsson H, Lalot S. Online fouling detection of domestic hot water heat exchangers. Heat Transfer Engineering, 2016; 37(15): 1231-1241. https://doi.org/10.1080/01457632.2015.1119584

[12] Davoudi E, Vaferi B. Applying artificial neural networks for systematic estimation of degree of fouling in heat exchangers. Chemical Engineering Research and Design, 2018; 130: 138-153. https://doi.org/10.1016/j.cherd.2017.12.017

[13] Ben-Mansour R, El-Ferik S, Al-Naser M, Qureshi BA, Eltoum MAM, Abuelyamen A, Ben Mansour R. Experimental/Numerical Investigation and Prediction of Fouling in Multiphase Flow Heat Exchangers: A Review. Energies, 2023; 16(6):2812. https://doi.org/10.3390/en16062812

[14] Zheng X, Yang R, Wang Q, Yan Y, Zhang Y, Fu J, Liu Z. Comparison of GRNN and RF algorithms for predicting heat transfer coefficient in heat exchange channels with bulges. Applied Thermal Engineering, 2022; 217:119263. https://doi.org/10.1016/j.applthermaleng.2022.119263

[15] Panda JP, Kumar B, Patil AK, Kumar M, Kumar R. Machine learning assisted modeling of thermohydraulic correlations for heat exchangers with twisted tape inserts. Acta Mechanica Sinica, 2023; 39(1): 322036. https://doi.org/10.1007/s10409-022-22036-x

[16] Kumra A, Rawal N, Samui P. Prediction of heat transfer rate of a Wire-on-Tube type heat exchanger: An Artificial Intelligence approach. Procedia Engineering, 2013; 64: 74-83. https://doi.org/10.1016/j.proeng.2013.09.078

[17] Wen XQ. Study on the Methods of Predicting the Fouling Characteristics of Plate Heat Exchanger Based on Water Quality Parameters. Applied Mechanics and Materials, 2014; 459: 153-158. https://doi.org/10.4028/www.scientific.net/AMM.459.153

[18] Wen X, Miao Q, Wang J, Ju Z. A multi-resolution wavelet neural network approach for fouling resistance forecasting of a plate heat exchanger. Applied Soft Computing, 2017; 57: 177-196. https://doi.org/10.1016/j.asoc.2017.03.043

[19] Aminian J, Shahhosseini S. Neuro-based formulation to predict fouling threshold in crude preheaters. International Communications in Heat and Mass Transfer, 2009; 36(5): 525-531. https://doi.org/10.1016/j.icheatmasstransfer.2009.01.020

[20] Kuzucanlı SA, Vatansever C, Yaşar AE, Karadeniz ZH. Assessment of fouling in plate heat exchangers using classification machine learning algorithms. In CLIMA 2022 conference, Rotterdam, Netherlands, May, 2022.

[21] Sundar S, Rajagopal MC, Zha H, Kuntumalla G, Meng Y, Chang H C, Salapaka S. Fouling modeling and prediction approach for heat exchangers using deep learning. International Journal of Heat and Mass Transfer, 2020; 159: 120112. https://doi.org/10.1016/j.ijheatmasstransfer.2020.120112

[22] Sun L, Zhang Y, Zheng X, Yang S, Qin Y. Research on the fouling prediction of heat exchanger based on support vector machine. International Conference on Intelligent

Computation Technology and Automation (ICICTA), China, 240-244, October, 2008. https://doi.org/10.1109/ICICTA.2008.156

[23] Sun L, Saqi R, Xie H. Research on the fouling prediction of heat exchanger based on wavelet relevance vector machine. Advances in Neural Network Research and Applications, 2010; 37-45. https://doi.org/10.1007/978-3-642-12990-2_5

[24] El-Said EM, Abd Elaziz M, Elsheikh AH. Machine learning algorithms for improving the prediction of air injection effect on the thermohydraulic performance of shell and tube heat exchanger. Applied Thermal Engineering, 2021; 185:116471. https://doi.org/10.1016/j.applthermaleng.2020.116471

[25] Shengxian C, Yanhui Z, Jing Z, Dayu Y. Experimental study on dynamic simulation for biofouling resistance prediction by least squares support vector machine. Energy Procedia, 2012; 17: 74-78. https://doi.org/10.1016/j.egypro.2012.02.065

[26] Harche R, Mouheb A. The fouling in the crude distillation preheat train of Algerian refinery. Acta Periodica Technologica, 2022;(53):272-284. https://doi.org/10.2298/APT2253272H

[27] Al-Naser M, Al-Toum M, El-Ferik S, Mansour RB, Al-Sunni F. Heat exchanger fouling prediction using artificial intelligence. In 5th International Conference on Advances in Mechanical Engineering, Istanbul, Turkey, 17-19, December, 2019.

[28] Al-Naser M, El-Ferik S, Mansour RB, AlShammari HY, AlAmoudi A. Intelligent Prediction Approach of Fouling Location in Shell and Tube Heat Exchanger. In 10th International Conference on System Engineering and Technology (ICSET), Shah Alam, Malaysia, 139-144, November, 2020. https://doi.org/10.1109/ICSET51301.2020.9265382

[29] Luo X, Patton AD, Singh C. Real power transfer capability calculations using multi-layer feed-forward neural networks. IEEE Transactions on Power Systems, 2000; 15(2): 903-908. https://doi.org/10.1109/59.867192

[30] Tabib SS, Jalali AA. Modelling and prediction of internet time-delay by feed-forward multi-layer perceptron neural network. In Tenth International Conference on Computer Modeling and Simulation (uksim), Cambridge, United Kingdom , 611-616, April, 2008. https://doi.org/10.1109/UKSIM.2008.93

[31] Bastani D, Hamzehie ME, Davardoost F, Mazinani S, Poorbashiri A. Prediction of CO2 loading capacity of chemical absorbents using a multi-layer perceptron neural network. Fluid Phase Equilibria, 2013; 354: 6-11. https://doi.org/10.1016/j.fluid.2013.05.017

[32] Leontaritis IJ, Billings SA. Input-output parametric models for non-linear systems part I: deterministic non-linear systems. International journal of control, 1985; 41(2): 303-328. https://doi.org/10.1080/0020718508961129

[33] Boussaada Z, Curea O, Remaci A, Camblong H, Mrabet Bellaaj N. A nonlinear autoregressive exogenous (NARX) neural network model for the prediction of the daily direct solar radiation. Energies, 2018; 11(3): 620. https://doi.org/10.3390/en11030620

[34] Mohanty S, Patra PK, Sahoo SS. Prediction of global solar radiation using nonlinear auto regressive network with exogenous inputs (narx). In 39th National Systems Conference (NSC), Greater Noida, India, 1-6, December, 2015. https://doi.org/10.1109/NATSYS.2015.7489103

[35] Pisoni E, Farina M, Carnevale C, Piroddi L. Forecasting peak air pollution levels using NARX models. Engineering Applications of Artificial Intelligence, 2009; 22(4-5): 593-602. https://doi.org/10.1016/j.engappai.2009.04.002

[36] Zibafar A, Ghaffari S, Vossoughi G. Achieving transparency in series elastic actuator of sharif lower limb exoskeleton using LLNF-NARX model. In 4th International Conference on Robotics and Mechatronics (ICRoM), Iran, 398-403, October, 2016. https://doi.org/10.1109/ICRoM.2016.7886771

[37] Bouaddi S, Ahmed I. Modeling and prediction of reflectance loss in CSP plants using a nonlinear autoregressive model with exogenous inputs (NARX). International Renewable and Sustainable Energy Conference (IRSEC), Marrakach, Moroco, 706-709, November, 2016. https://doi.org/10.1109/IRSEC.2016.7984071

[38] Alabi KO, Abdulsalam SO, Ogundokun RO, Arowolo MO. (2021). Credit risk prediction in commercial bank using chi-square with SVM-RBF. In Information and Communication Technology and Applications: Third International Conference (ICTA), Minna, Nigeria, 158-169, November 24-27, 2020. https://doi.org/10.1007/978-3-030-69143-1_13

[39] Khemakhem S, Boujelbene Y. Artificial intelligence for credit risk assessment: artificial neural network and support vector machines. ACRN Oxford Journal of Finance and Risk Perspectives, 2017; 6(2):1-17.

[40] Reddy SVG, Reddy KT, Kumari VV, Varma KV. An SVM based approach to breast cancer classification using RBF and polynomial kernel functions with varying arguments. International Journal of Computer Science and Information Technologies, 2014; 5(4): 5901-5904.

[41] Amiri B, Dizène R, Dahmani K. Most relevant input parameters selection for 10-min global solar irradiation estimation on arbitrary inclined plane using neural networks. International Journal of Sustainable Energy, 2020; 39(8): 779-803. https://doi.org/10.1080/14786451.2020.1758104

[42] Dahmani A, Ammi Y, Hanini S, Redha Yaiche M, Zentou H. Prediction of Hourly Global Solar Radiation: Comparison of Neural Networks/Bootstrap Aggregating. Kemija u industriji: Časopis kemičara i kemijskih inženjera Hrvatske, 2023; 72(3-4): 201-213. https://doi.org/10.15255/KUI.2022.065

[43] Garson GD. (1991). Interpreting neural-network connection weights. AI expert, 1991; 6(4): 46-51.

[44] Goh AT. Back-propagation neural networks for modeling complex systems. Artificial intelligence in engineering, 1995; 9(3): 143-151. https://doi.org/10.1016/0954-1810(94)00011-S

[45] Hosseini S, Khandakar A, Chowdhury ME, Ayari MA, Rahman T, Chowdhury MH, Vaferi B. Novel and robust machine learning approach for estimating the fouling factor in heat exchangers. Energy Reports, 2022; 8: 8767-8776. https://doi.org/10.1016/j.egyr.2022.06.123

[46] Tong S, Zhang X, Tong Z, Wu Y, Tang, N, Zhong W. Online ash fouling prediction for boiler heating surfaces based on wavelet analysis and support vector regression. Energies, 2019;13 (1):59. https://doi.org/10.3390/en13010059

[47] Jradi R, Marvillet C, Jeday MR. Analysis and estimation of cross-flow heat exchanger fouling in phosphoric acid concentration plant using response surface methodology (RSM) and artificial neural network (ANN). Scientific Reports, 2022; 12(1): 20437. https://doi.org/10.1038/s41598-022-24689-2

[48] Tang SZ, Li MJ, Wang FL, He YL, Tao WQ. Fouling potential prediction and multi-objective optimization of a flue gas heat exchanger using neural networks and genetic algorithms. International Journal of Heat and Mass Transfe r, 2020; 152: 119488. https://doi.org/10.1016/j.ijheatmasstransfer.2020.119488

[49] Kashani MN, Aminian J, Shahhosseini S, Farrokhi M. Dynamic crude oil fouling prediction in industrial preheaters using optimized ANN based moving window technique. Chemical Engineering Research and Design, 2012; 90(7): 938-949. https://doi.org/10.1016/j.cherd.2011.10.013